THE CORNELL HIGH-CURRENT ERL INJECTOR CRYOMODULE*

M. Liepe[†], S. Belomestnykh, E. Chojnacki, Z. Conway, V. Medjidzade, H. Padamsee, P. Quigley, J. Sears, V. Shemelin, V. Veshcherevich, CLASSE, Cornell University, Ithac, NY, U.S.A.

Abstract

Cornell University has developed and fabricated a SRF injector cryomodule for the acceleration of the high current (100 mA), low emittance beam in the Cornell ERL injector prototype. This cryomodule is based on superconducting rf technology with five 2-cell rf cavities operated in the cw mode. To support the acceleration of a low energy, ultra low emittance, high current beam, the beam tubes on one side of the cavities have been enlarged to propagate Higher-Order-Mode power from the cavities to broadband RF absorbers located at 80 K between the cavities. Each cavity is surrounded by a LHe vessel and equipped with a frequency tuner including piezo-driven tuners for fast frequency control. The cryomodule provides the support and precise alignment for the cavity string, the 80 K cooling of the HOM loads, and the 2 K LHe cryogenic system for the high cw heat load of the cavities. In this paper results of the commissioning phase of this cryomodule will be reported.

INTRODUCTION

Cornell University's Laboratory for Accelerator based Sciences and Education is currently exploring the potential of a x-ray light source based on the Energy-Recovery-Linac (ERL) principle [1], which promises superior X-ray performance as compared to conventional third generation light sources [2]. As a first step, to study and demonstrate the production and preservation of a high current, ultra-low emittance beam, a prototype of the ERL injector has been developed and constructed, see Figure 1. One of the most challenging and critical components in the injector is its superconducting radio-frequency (SRF) cryomodule, hosting five SRF 2-cell 1.3 GHz cavities. The cavities in the module are powered by individual high power (120 kW) CW klystrons, located on a mezzanine above the injector prototype. Extensive infrastructure required to operate this cryomodule has been installed, including the cryogenic refrigerator, high power klystrons, and a digital LLRF control system, see Figure 2. The installation of the injector components was finished in April 2008. The first commissioning and beam operation period stated in June 2008, and ended in August 2009 [3]. Currently, parts of the ERL injector, including its cryomodule, are being re-worked to address several issues found during the first run period. Beam operation will resume early 2010.

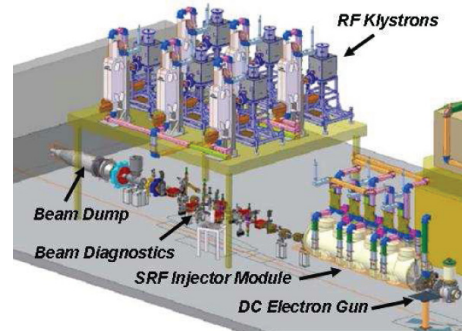In the following we will first give a short summary of beam

Figure 1: Layout of the ERL injector prototype.

Figure 2: Left: 120 kW CW klystrons. Right, top: Cryogenic pumps. Right, bottom: LLRF control hardware.

results from the first run period. The main part of this paper will then focus on the ERL injector cryomodule. We will discuss module design and assembly, followed by detailed results from the commissioning and performance testing of the injector module. We will end by giving an overview of the ongoing re-work of the ERL injector cryomodule.

OVERVIEW OF BEAM RESULTS FROM THE FIRST RUN PERIOD

During the first run period of the ERL injector extensive commissioning and testing of all main components was done. Several important milestones where achieved, but also some issues where found that need to be addressed before ultimate performance of this injector can be reached. The DC photo gun is operational since 2006. Excellent vacuum has been demonstrated, which is essential for good photo cathode lifetime. Gap voltages of up to 425 kV have been achieved, close to the design goal of 500 kV. Field emission at higher voltages however did cause a ce-
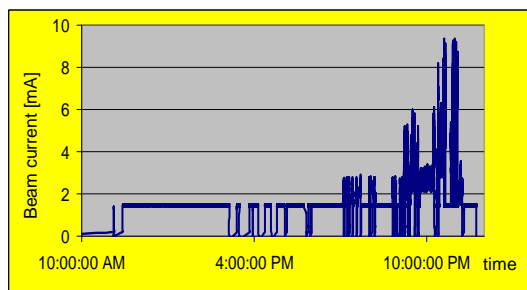
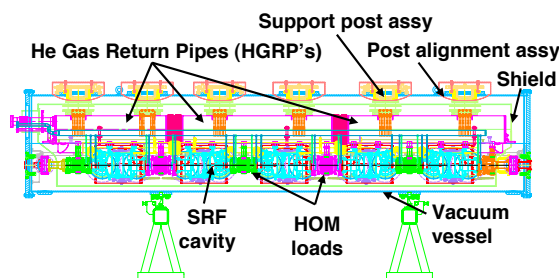Figure 3: Beam current during high current operation.

Figure 4: Longitudinal cross-section of the ERL injector module with 5 SRF cavities with HOM beam line absorbers in between. The module is longitudinally separated in three sections, each supported and aligned independently.

ramic puncture, and operation was limited administratively to 250 kV after repair. Further, stability of the gun laser system and the gun high voltage power supply were studied in detail, and some improvements are needed for future high beam current operation. While the main focus during the first run period was on commissioning and low bunch charge operation, high beam current was also explored. Figure 3 shows the beam current history during one of the high beam current operations. Beam currents of above 8 mA have been achieved, limited primarily by beam loss due to insufficient stability of some of the beam parameters at higher currents, as mentioned above. At low bunch charges, normalized emittances in both planes after the cryomodule (i.e. at 5 MeV) have been found to be close to the thermal limit at the cathode for the given laser size (0.2 to 0.4 mm mrad). Refer to [3] for a detailed discussion of the beam results. Resolving the limitations found during the first beam operation period is the goal of the current injector re-work, and includes installation of a new high voltage gun ceramics with bulk conductivity, improving the stability and power handling of the laser system, improving the control circuit stabilizing the gun high voltage, as well as addressing two issues found during testing the injector cryomodule, as discussed below.

MODULE DESIGN AND INNOVATIONS

The ERL injector cryomodule design is based on the TTF cryomodule [4], with beam line components supported from a large diameter helium gas return pipe (HGRP) and all cryogenic piping located inside the module. This concept has been significantly redesigned to fulfill ERL specific requirements, which include (1) the acceleration of a high current beam with up to 500 kW of total power transferred to the beam, (2) significant Higher-Order Mode (HOM) power extraction from the SRF cavities, (3) the preservation of the ultra-low emittance of the electron beam, and (4) CW cavity operation with high cryogenic loads. Table 1 lists some of the key specifications of the injector cryomodule. This module also serves as a conceptual prototype for ERL main linac [5]. Key features and innovations of the injector prototype cryomodule include among

Table 1: ERL injector cryomodule specifications.

Numb. of cavities / HOM loads	5 / 6
Accelerating voltage per cavity	1 - 3 MV
Fundamental mode frequency	1.3 GHz
R/Q (circuit definition) per cavity	111 Ohm
Loaded quality factor	4.6×10^4 to 10^6
RF power installed per cavity	120 kW
Required amplit. / phase stab. (rms)	1×10^{-3} / $0.1°$
Maximum beam current (design)	100 mA
Total 2K / 5K / 80K loads	$\approx$ 26 / 60 / 700 W
Overall length	5.0 m

others (see also Fig. 4 and Table 1): (1) A symmetric beamline avoids transverse on-axis fields, which would cause emittance growth. (2) The 2K, 4.5K, and 80K cryogenic systems in the module have been upgraded to intercept the high dynamic heat loads. (3) Three magnetic shield layers effectively shield external magnetic fields. (4) Only one layer of thermal shield (at 80K) is used. (5) Short module end sections minimize the distance between the photo-emission DC gun and the first cavity. (6) Gate-valves on each module end, located inside of the module with their drive units outside of the module, make external gate vales obsolete. (7) A new cavity string alignment concept simplifies module assembly and provides improved alignment tolerances. In this concept, the cavities and HOM loads are mounted via precisely machined, fixed supports to the HGRP sections. The alignment of the cavities can be improved even further by adjusting the cavity positions via alignment bolts at the HGRP support posts once the module is cold. Refer to [6] for details on the module design.

MODULE ASSEMBLY

Prototypes of the main beam line components (cavities, HOM loads, input couplers) have been developed, fabricated and tested individually [7, 8, 9]. Following the suc-
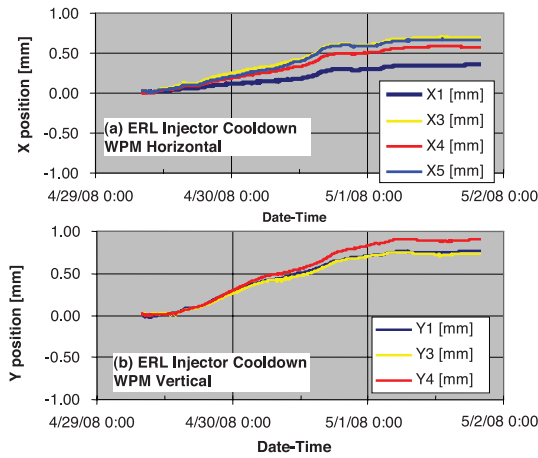
Figure 5: WPM data during cool-down of the injector module. Top: Horizontal position of WPM blocks on cavities 1, 3, 4, and 5. Bottom: Vertical position of WPM blocks on cavities 1, 3, and 4. WPM #2 is not functional.

cessful full system test of a one cavity horizontal test cryomodule [10], the full ERL injector SRF cryomodule has been fabricated and assembled; refer to [11] for details. In May 2008, the injector module was installed in the ERL injector, cooled down to 2K, and commissioning started.

COOL DOWN AND ALIGNMENT

The cryomodule was cooled down from room temperature to 4.2 K over a period of 2.5 days. Above 80K, the cool-down rate was limited to < 10K/hour to reduce thermal stress. No problems or leaks were found during module cool-down. Fundamental mode frequencies of all cavities were measured after cool-down. Prior to any cavity tuning, a frequency spread of only 17 kHz was found. During cool-down, the shift in cavity positions was monitored by a wire-position-monitor (WPM) system. To each cavity, a WPM block is directly mounted for measuring the horizontal and vertical positions of the cavities independently, see Figure 5. The observed position shifts during cool-down are in very good agreement (within 0.2 mm) with values expected from thermal shrinkage of the cavity support structure and of the WPM block support. After cool down, the maximum transverse alignment errors of the SRF cavities in the injector module are ± 0.2 mm. Such excellent cavity string alignment is important for emittance preservation of the low energy beam in the ERL injector.

STATIC HEAT LOAD AND CRYOGENICS

The static heat leak to 1.8K was measured by closing the JT valve in the LHe feed and measuring the LHe boil-off rate. Heaters on the 1.8K system were used for calibration. These measurements give a static heat leak to 1.8K of 13 ± 4 W, in good agreement with the expected static 1.8K load of 10 W. The dominating part of this static heat load comes from thermal conduction from "4.5K intercepts" in the in-

put couplers, support posts and HOM absorbers to the 1.8 K system. Currently, the "4.5K system" of the cryomodule is cooled by high pressure helium gas at an elevated temperature of about 6K as a result of non-ideal heat exchange in the refrigerator system, which increases the estimated total 1.8K static load from 5 W to 10 W.

The pump skids installed can provide a heat removal capacity of about 130W at 2 K, or 23 W of dynamic heat load per cavity. This is above the measured heat transfer limit through the LHe in the "chimneys" on top of the LHe tanks around the individual cavities, which is ≈ 15 W at 2K. The resulting maximum heat flux of 1.2 W/cm^2 at 2K is in very good agreement with values found in literature.

RF SYSTEM

The injector cryomodule RF system employs five klystrons, each delivering up to 120 kW of CW RF power to individual cavities via twin input couplers [7, 12]. The 7-cavity K3415LS tube manufactured by e2v has a saturated output power of about 160 kWCW. To provide stable regulation of the cavity field, the klystron must have a non-zero gain and therefore cannot operate in saturation. The klystrons passed the factory acceptance test meeting specifications at 135 kW before shipping. The tubes were installed, tested again at Cornell, and are preforming well. Figure 6 shows typical transfer curves of the e2v klystrons, with efficiencies exceeding 50% above 120 kW output power. The commissioning of the injector RF system is described in detail in [13].

INPUT COUPLER

All high power RF twin-input couplers have so far been processed up to 50 kW under full refection, see Figure 7. All couplers conditioned well, reaching these power levels in pulsed operation within 25 to 75 hours of processing (RF on time). None of the input coupler parts were baked after assembly to the beam line. The warm part of the couplers can be baked in situ via heating elements installed on the couplers in the module, if it should be required to reach power levels above 50 kW.
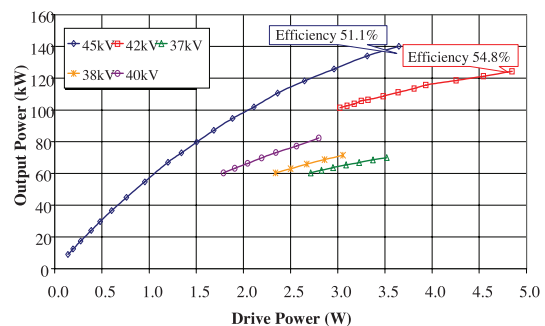

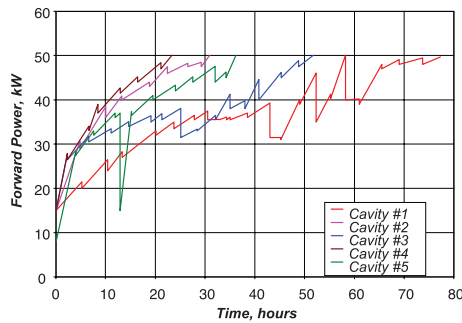Figure 6: Transfer curve of the ERL injector klystron.

Figure 7: Input coupler processing under full refection (cavity detuned) up to 50 kW. Shown is the maximum forward power per twin-coupler vs. processing time (pulsed operation with 2 ms pulse length and 50 Hz repetition rate).

SRF CAVITY PERFORMANCE

All 5 SRF cavities in the injector cryomodule have been performance tested individually at 1.8K to 2K, see Figure 8 and Table 2. In CW mode all cavities reached accelerating voltages of at least 2.8 MV when powered individually (limited by heat flux in the LHe bath), close to the maximum specification of 3 MV. All cavities show field emission at higher fields, and cavity processing was done on some of the cavities to further increase maximum field gradients. All cavities also show low intrinsic quality factors below 10^{10} at 2K even at low fields. Note that the cavities on both ends of the module have the lowest Q values. Early cavity Q measurements shortly after module cool down indicated that the intrinsic quality factors started out around 10^{10}, and then might have degraded over time. This is also supported by two measurements of the effective intrinsic quality factor of all 5 cavities operated together, see Figure 9. The two measurements have been spaced in time by several months, and show a further reduction in the intrinsic quality factors of the cavities. As of writing the cause of these low quality factors is still unknown. As discussed below, the injector cryomodule has been disassembled recently, and the individual cavities are currently vertically tested to investigate the cause of the low quality factors. First results indicate no dust contamination, but hydrogen disease was found on a spare cavity which had received the same surface treatment as the cavities in the injector module. Other potential causes may include losses in the beam tube and coupler regions (the cavity flanges are thermally anchored to the "4.5K" cooling circuit, which was elevated at a temperature of 6K; this significantly increases the BCS surface resistance in the cavity end regions), cryo-pumping of residual gases, or multipacting.

HIGHER-ORDER MODES

The Higher-Order Mode absorbers located at 80K between the SRF cavities allow for measuring the total HOM power excited by the beam. At the design bunch charge (77 pC) and high beam current (100 mA), > 200 W of

Table 2: Cavity Performance. (IC: Input coupler vacuum.)

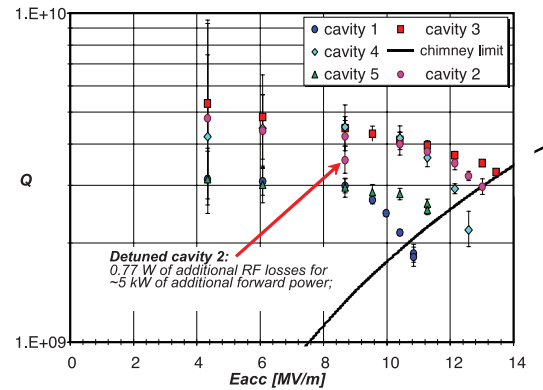| Cavity	CW	Limit	Pulsed	Limit
1	2.8 MV	Cryogenics	4.4 MV	IC
2	3.0 MV	Cryogenics	5.5 MV	IC
3	3.5 MV	Cryogenics	3.7 MV	IC
4	3.4 MV	Cryogenics	4.2 MV	Quench
5	2.8 MV	Quench	5.3 MV	Quench
all	2.4 MV	Cryogenics	-	-

Figure 8: Intrinsic quality factor of the five 2-cell injector SRF cavities as a function of accelerating field gradient at 2K. Also show is the 1 W/cm^2 heat flux limit for the LHe in the chimney connecting the LHe tank around the cavity to the 2K-2 phase LHe supply line.

HOM power will be extracted at the HOM absorbers [14]. Heaters mounted on the HOM load bodies are used to calibrate the increase in temperature of the He cooling gas of the loads as a function of power absorbed in each HOM load, see Figure 10. However, the maximum beam current passed thought the injector module so far was limited to ≈ 8 mA with 6 pC bunches. The expected HOM power exited by such a beam is only a few 100 mW per cavity,
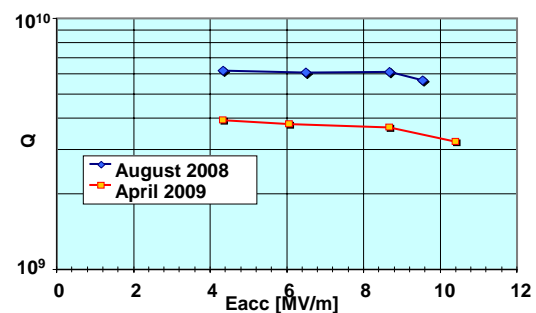

Figure 9: Effective intrinsic quality factor of all five 2-cell injector SRF cavities operated together as a function of accelerating field gradient at 2K. Shown are two measurements, spaced in time by 8 months.
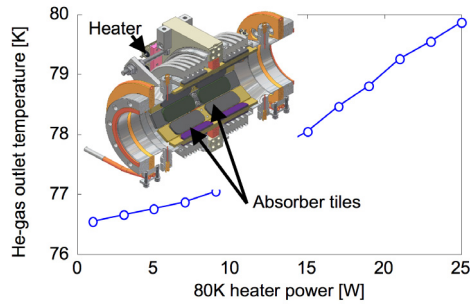
Figure 10: Measured temperature increase of the 80K He outlet gas vs. HOM heater power during calibration.

which is too low to be detected. The damping of HOMs in the injector cavities by the beamline absorbers was investigated using a vector network analyzer to excite modes via pick-up antennas located at the cavity beam tubes and at the HOM loads, see Figure 11. Preliminary results confirm very strong suppression of monopole and dipole modes with typical quality factors of only a few 1000.

LLRF FIELD CONTROL

The LLRF electronics for the ERL injector is a improved generation of LLRF system previously developed for CESR [15], with lower loop latency $< 1\mu$s and increased sample rates and ADC resolution (16 bits). Integral and proportional gains of the PI loop used to stabilize the RF fields in the cavities have been optimized, as shown in Figure 12 and 13. At optimal gains, exceptional field stabilities of $\sigma_A/A < 2 \times 10^{-5}$ in relative amplitude and $\sigma_p < 0.01°$ in phase (in-loop measurements) have been achieved, far exceeding the ERL injector and ERL main linac requirements. The main source of field perturbation in the injector cavities is a strong ripple on the high voltage of the klystrons, with relative amplitudes of several percent and frequencies ranging from 360 Hz to may kHz.
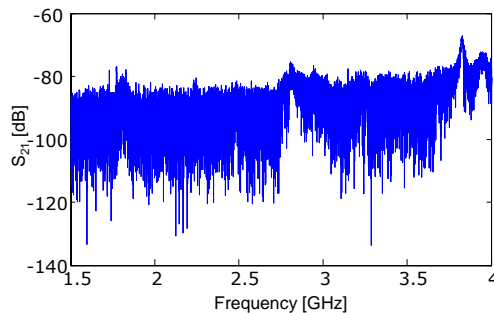

Figure 11: Vector network analyzer scan for HOMs between 1.5 GHz to 4 GHz. Shown is the transmission amplitude vs. scan frequency. Pick-up antennas on the cavities and HOM loads where used to couple to the HOMs.
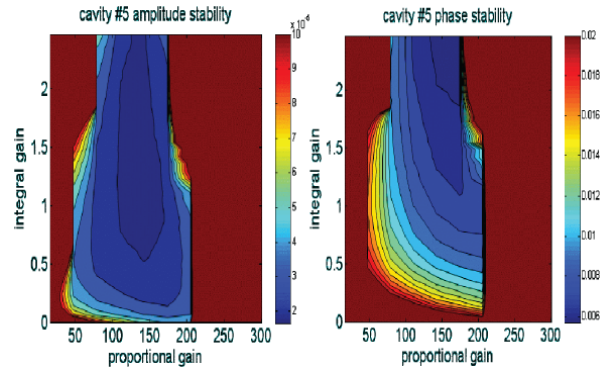
Figure 12: Integral and proportional gain scan to optimize the gains used in the field control loop. Left: Amplitude stability (blue: $\sigma_A/A < 2 \times 10^{-5}$). Right: Phase stability (blue: $\sigma_p < 0.01°$).

CAVITY DETUNING

Though cavity microphonics are not a concern for the ERL injector with its low loaded quality factor cavities, it will be the main field perturbation source in the ERL main lianc, and will determine the RF power required to operate these cavities. Extensive studies on microphonics, its sources and coupling to the SRF cavities, and active detuning compensation have been started therefor on the ERL injector module as a testbed [16, 17]. Typical microphonics levels of a few Hz rms have been found (Figure 14) with significant differences between individual cavities and significant changes over time. Measurements with dynamic sinusoidal forces exerted by a modal shaker on various external parts of the cryomodule (module support, waveguides, beamline, cryolines) show that ground vibrations and other mechanical vibrations do not strongly couple to the SRF cavities, indicating that the major contribu-
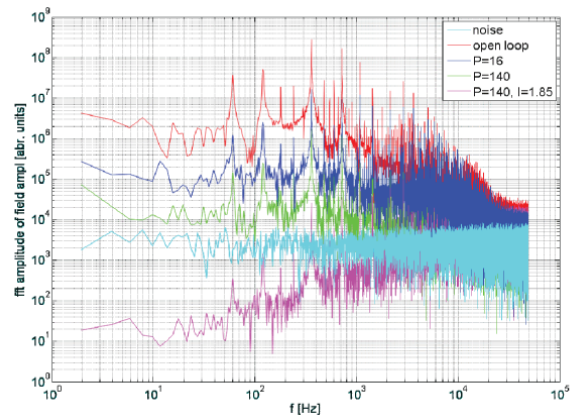

Figure 13: FFT amplitude spectrum of the cavity RF field amplitude for different gain settings. Also shown is the noise spectrum without input connected to the 50 MHz, 16 bit ADC used in sampling the RF field, corresponding to an integrated rms fluctuation of 0.1 bits for f< 50 kHz.
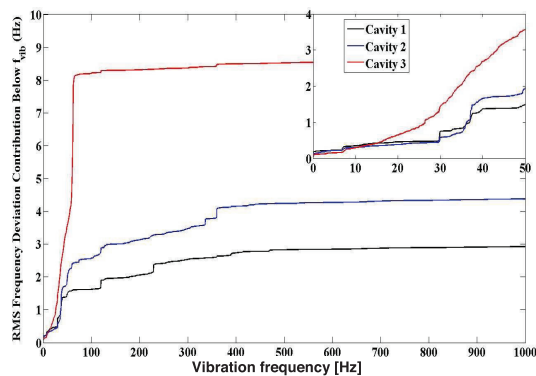
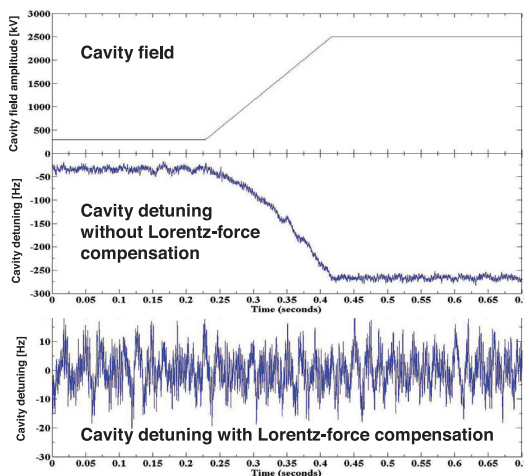Figure 14: The integrated microphonic spectra for three different cavities in the ERL injector module.

Figure 15: Top: The cavity field is ramped up to 2.5 MV in 0.2 seconds. Middle: Lorentz-force detuning without active compensation. Bottom: Cavity detuning during field ramp up with active detuning compensation.

tion to cavity microphonics comes from fast fluctuations in the sub atmospheric He-pressure and the cryogenic system. Lorentz-force detuning has been compensated reliably using the fast piezoelectric actuators implemented in the cavity frequency tuners in a feedback loop (Figure 15). The motor driven frequency tuner (adapted from the blade tuner design [18]) show good linearity with a frequency resolution of about 2 Hz per step.

ABSORBER TILE CHARGING

In a search for residual fields along the beam axis in the injector module, a very low energy beam was passed through the module. Its transverse position was measured using beam deflections by RF kick fields excited in the coupler regions of the beam pipe with low RF power, while the cavities where detuned strongly, see Figure 16. Detuning the cavities in these measurements by many bandwidths ensured that the fields inside the cavities are small and the change in beam energy is negligible. The beam trajectory obtained this way shows the presence of resid-
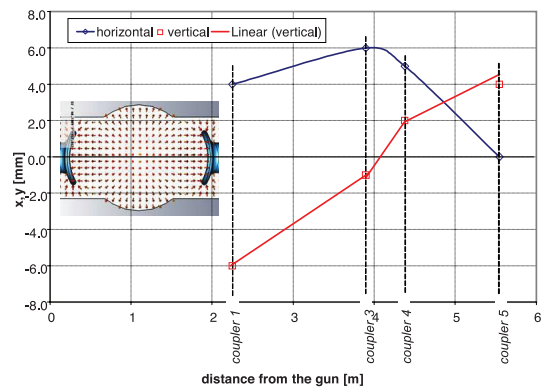
Figure 16: Orbit of a very low energy (250 keV) beam in the injector cryomodule as estimated by measuring transverse kicks by the RF fields in the input coupler regions. The RF field is exited by a forward power (< 1 kW) with strongly detuned cavities. The resulting electric RF field has a quadrupole like pattern. By measuring magnitude and direction of the kick to the beam at a given forward power, the beam position in the coupler region can be determined.

ual stray fields between cavities 2 and 3, as well as 3 and 4. Additional kick scans with a DC voltage applied between the inner conductors of the twin input couplers (up to 1000 V), confirmed the presence of stray fields in these regions. Initially, residual magnetic fields where suspected as the cause of the beam deflections. The cryomodule was warmed up to room temperature, and access ports at the side of the module where opened to search for regions of magnetic fields above a few 10 mG inside the module (between cavities). No areas of elevated magnetic fields where found near the beam line. Nevertheless, the suspected areas of stray fields where demagnetized in-situ. After cool down the stray fields where gone, but reappeared after a few days of beam operation. Subsequently, the cause of these beam deflections was found to be charging up of some of the absorber tiles at 80K in the HOM loads (see Figure 10) by small beam losses, thereby generating kV scale electric fields on the beam axis. DC resistivity measurements confirmed very high resistivities at cryogenic temperatures of some of the absorber materials used in the HOM loads (see Figure 17), resulting in discharging time constants of several hours to days [19].

CRYOMODULE RE-WORK

Starting in September 2009, the injector cryomodule was partly dissembled. This re-work of the module will focus on re-processing the SRF cavities to improve their intrinsic quality factors and on eliminating the charging up of the absorber tiles by beam loss. We are currently exploring several potential solutions for the absorber charging problem including (1) coating the absorber tiles with a very thin conducting layer, and (2) removing all absorber tiles facing the beam, leaving only tiles tiles facing outwards, which are shielded from the beam; see Figure 18. The low energy
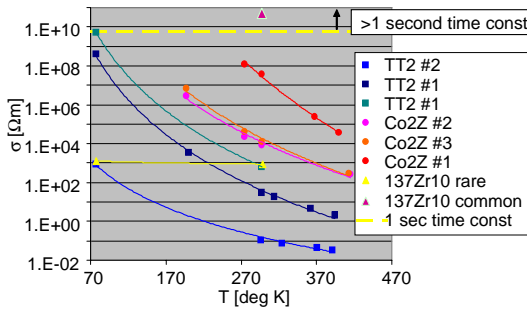
Figure 17: Resistivity of RF absorber materials and the threshold for 1 second time constant.

Figure 18: Left: EB-welder setup to study absorber tile charging. Middle: DC resistivities. Right: Elkonite support plate after cutting off the inner facing absorber tiles.

beam in an electron beam welder is used to further study the charging of the tiles and the resulting beam deflection as shown in Figure 18, left. In addition, stress relieving cuts will be added to the absorber plates to further reduce thermal stresses on the absorber tiles during cool down, see Figure 19. We are also exploring new absorber materials with sufficient DC conductivity. For example, we found that Carbon nano-tubes (CNT) in alumina ceramic show strong, broadband RF absorption [20]. Figure 20 shows the complex permittivity of this material. After reassembly of the cryomodule, beam tests will resume early 2010.

Figure 19: Top: Elkonite plate with stress relieve cuts at the ends of the 4 ferrite tiles. Middle: Deflection due to thermal contraction during cool down (strongly exaggerated). Bottom left: Stresses in the absorber plate after cool down.
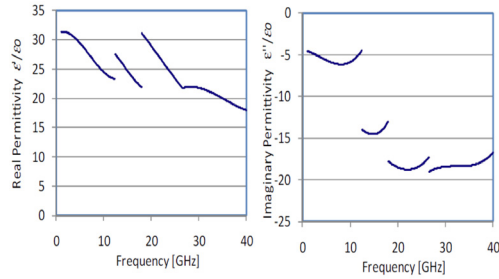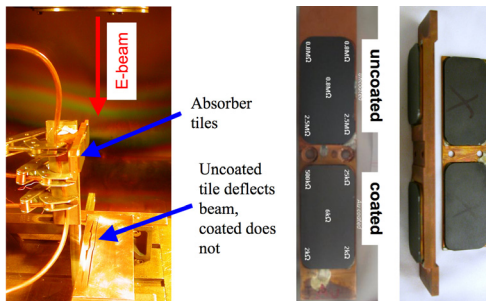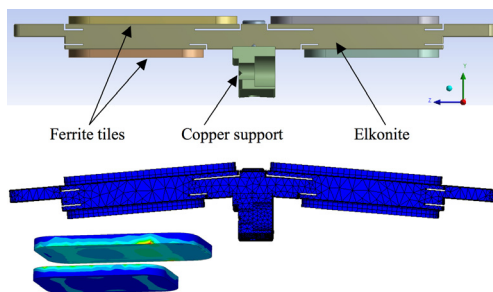

Figure 20: Real part (left) and imaginary part (right) of permittivity in the 1-40GHz range for alumina nanocomposites with 1% weight multi-wall carbon nanotubes.

REFERENCES

[1] J. A. Crittenden et al.,"Developments for Cornells...", PAC'09, Vancover, May 2009, paper MO4PBC03 (2009).

[2] D. H. Bilderback, Proceeding of Future Light Sources 2006 meeting in Hamburg, PLT03, p1-6 (2006).

[3] I. Bazarov et al., PAC'09, Vancover, May 2009 (2009).

[4] C. Pagani et al., Advances in Cryogenic Engineering, Vol. 45A, Edited by Q-S. Shu, Plenum Press, New York (1999).

[5] E. Chojnacki, et al., "Design of an ERL Linac Cryomodule," PAC'09, Vancover, May 2009 (2009).

[6] M. Liepe et al., "Design of the CW Cornell ERL Injector Cryomodule," PAC'05, Knoxvill, TN, USA (2005).

[7] V. Veshcherevich, et al., "Design of High Power Input Coupler...," Proc. of SRF'2005 Workshop (2005).

[8] V. Shemelin, et al., "Dipole-mode-free and kick-free 2-cell Cavity...," Proc. of PAC'03, pp. 2059-2061 (2003).
R. L. Geng, et al., Proc. of PAC'07, pp. 2340-2342 (2007).

[9] V. Shemelin et al., EPAC 2006, Edinburgh, Scotland (2006).
V. Shemelin al., NIM A 557 (2006) 268-271.

[10] S. Belomestnykh et al., "First Test of the Cornell Single-cavity...," EPAC08, Genoa, Italy, paper MOPP117, (2008).

[11] E. Chojnacki et al., EPAC08, Genoa, Italy, p. 844 (2008).

[12] S. Belomestnykh, et al., "Development of High RF Power Delivery...," LINAC'2004, pp. 694-696 (2004).

[13] S. Belomestnykh et al., "Commissioning of the Cornell ERL...," EPAC08, Genoa, Italy, paper MOPP116, (2008).

[14] W. Russel and M. Liepe, "Wakefields in the Cornell ERL Injector," SRF 2009, Berlin, paper THPPO004, (2009).

[15] M. Liepe et al., PAC'03, Portland, Or, USA (2003).

[16] Z. Conway, M. Liepe, "Electromagnetic and mechanical properties...," PAC'09, Vancover, May 2009 (2009).

[17] Z. Conway, M. Liepe, "Fast piezoelectric actuator control of microphonics...," PAC'09, Vancover, May 2009 (2009).

[18] C. Pagani, "SRF Activities at INFN Milano - Lasa", 10th Workshop of RF Superconductivity, Tsukuba, Japan (2001).

[19] E. Chojnacki et al., "DC Conductivity of RF Absorbing Materials," SRF 2009, Berlin, paper THPPO035, (2009).

[20] E. Chojnacki et al., "Carbon Nanotube RF Absorbing Materials," SRF 2009, Berlin, paper THPPO036, (2009).

01 Progress reports and Ongoing Projects